CHIRALITY 21:S242–S252 (2009)

Review Article

NIR-VCD, Vibrational Circular Dichroism in the Near-Infrared: Experiments, Theory and Calculations

SERGIO ABBATE,[1,2]* ETTORE CASTIGLIONI,[1,3] FABRIZIO GANGEMI,[1,2] ROBERTO GANGEMI,[1,2] AND GIOVANNA LONGHI[1,2]

[1]*Dipartimento di Scienze Biomediche e Biotecnologie, Università di Brescia, 25123 Brescia, Italy*
[2]*Consorzio Nazionale Interuniversitario per le Scienze Fisiche della Materia, 00146 Roma, Italy*
[3]*Jasco Corporation, 2967-5 Ishikawa-cho, Hachioji-shi, Tokyo 192-8537, Japan*

Contribution to the Special Thematic Project "Advances in Chiroptical Methods"

ABSTRACT The first well documented experiments of Near Infrared Vibrational Circular Dichroism (NIR-VCD) were performed around 1975. We review the thirty year history of NIR-VCD, encompassing both instrumental development and theoretical/computational methods that allow interpretation of experimental spectra, harvesting useful structural information therefrom. We hope to stimulate interest in this still scarcely explored spectroscopy of chiral molecules. *Chirality 21:S242–S252, 2009.* © 2009 Wiley-Liss, Inc.

KEY WORDS: NIR; VCD; overtones and combinations; local modes; mechanical anharmonicity; electrical anharmonicity

INTRODUCTION

Near Infrared (NIR) absorption spectroscopy has emerged during the last 25 years as one of the most useful and indeed used techniques for quality control, process and analytical controls in various industries,[1] such as pharmaceutical and food industry. In the industrial application of this technique, dedicated commercial analyzers are employed and NIR spectra are not interpreted at molecular level but are elaborated with statistical tools. In parallel and independently, the local mode interpretation of NIR and visible vibrational absorption spectra has provided a first grip onto the fundamental mechanisms governing vibrational overtone absorption of light[2–5]; recently, an interesting application of the latter studies has been provided in the investigation of the earth atmosphere.[6]

In the same years, Circular Dichroism (CD) and in particular Vibrational Circular Dichroism (VCD), which is CD due to vibrational transitions in the IR range, has demonstrated quite efficacious in the study of configurational and conformational properties of chiral molecules. CD is the form of spectroscopy that studies the difference in the absorption of left and right circularly polarized light as function of wavelength (or wavenumber). VCD measurements in the NIR range were also effected in this period: we mention in particular the much cited work of Keiderling and Stephens in 1976,[7] reporting data relative to the first CH stretching overtone and to the first CH stretching/HCH bending combinations. Since then several other experiments have been performed, not in many labs though, and higher overtones have been investigated too.

We review here for the first time the experimental work. We hope in this way that the industrial labs mentioned at the beginning of this article will find NIR-VCD an interesting technique, and will give the needed impulse to this form of spectroscopy. They should become convinced that this new spectroscopy allows study of "dark" compounds, that is to say those with no UV-Vis chromophore, with chirality embedded. NIR-VCD may prove advantageous also because of easy sample preparation. So far just liquids and solutions have been examined in normal quartz cuvettes, in contrast to what happens in IR-VCD, where minimal quantities of substance have to be used with very difficult-to-handle cells. In the future, solid samples or pellets should also be considered, as it is being increasingly requested by the food industry and by the pharma industry. In part III of the manuscript we consider also the status of theory and calculations, especially those employing ab-initio methods, that permit attainment of a full understanding of the vibrational features and their manifestation in NIR-VCD. Only with reliable calculations of the predicted spectra one could use data to gain information on Absolute Configuration and/or Molecular Conformations, as already practiced in mid-IR VCD.

EXPERIMENTS

The modern standard approach to CD originated with the introduction of the circular polarization modulator, which was patented in France in 1960.[8] The materials

Fabrizio Gangemi is currently at DIBIT San Raffaele Scientific Institute, Via Olgettina 58, 20132 Milano, Italy.
*Correspondence to: Sergio Abbate, Dipartimento di Scienze Biomediche e Biotecnologie, Università di Brescia, Viale Europa 11, 25123 Brescia, Italy. E-mail: abbate@med.unibs.it
Received for publication 24 April 2009; Accepted 9 September 2009
DOI: 10.1002/chir.20805
Published online 19 November 2009 in Wiley InterScience (www.interscience.wiley.com).

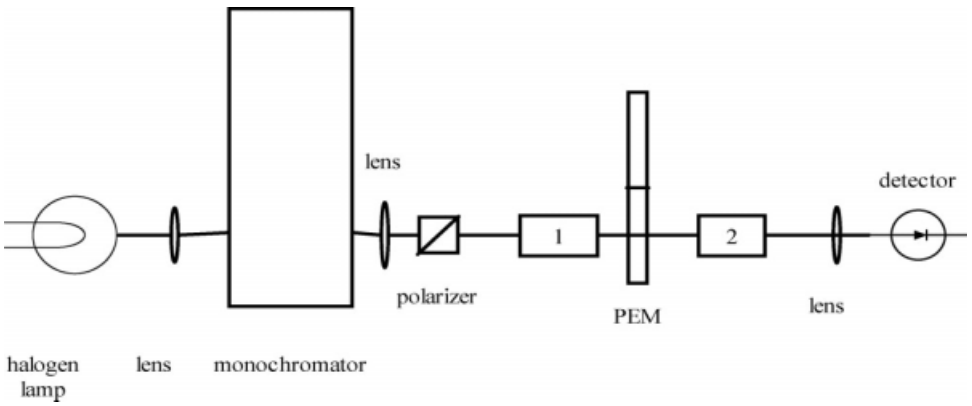

Fig. 1. Scheme of the apparatus for measuring NIR-VCD in Brescia.

used in this device, the Pockels cell modulator, KDP (= KH_2PO_4) and ADP (= $NH_4H_2PO_4$), restricted the wavelength range to the UV-Vis region, since the high voltage necessary to obtain quarter-wave retardation in the NIR would destroy the crystal.

NIR CD was first measured by Abu-Shumays and Cook[9] and by Eaton and Lovenberg[10] in 1970 with homemade dedicated instruments and by more conventional approaches. They made use of the rotating polarizer Fresnel crystal system, first applied in Norwich[11] by modifying a commercial double-beam UV-Vis-NIR spectrophotometer, with differently oriented polarizers and Fresnel prisms or mica retardation plates. The first three NIR-extended CD spectrometers based on the use of photoelastic modulators (PEM), which were able to provide quarter-wave retardation over the whole range, were announced almost simultaneously (1972) in Paris,[12] Chicago[13] and Los Angeles.[14] All these units contained a rotating chopper to further modulate the light beam as required by IR detectors; the first two were targeted at CD in the standard IR (VCD), whereas the last one was developed mainly for measuring Magnetic Circular Dichroism (MCD) of electronic transitions. The first vibrational CH-stretching overtone CD measurements were reported in 1976[7] and were obtained with a modified version of this last instrument. The following years have seen other units proposed in the US[15] and in Japan.[16] The instrument assembled in Japan was a prototype; subsequently made into a commercial unit by JASCO and named J-200D, it was sold worldwide mainly for MCD applications. With a spectrometer of this type the second and third vibrational CH-stretching overtones were measured in 1989.[17] We wish to mention that for the latter instrument two detectors, a regular photomultiplier tube and a liquid N_2-cooled InSb detector, allowed coverage of the 2000–500 nm range.

The third article dealing with CH-stretching overtone CD appeared in 1994, using a homemade unit based on a Ti-sapphire tunable laser.[18] Several other NIR CD spectrometers, mainly oriented to MCD applications, were presented in those years, and we just wish to mention the synchrotron based unit developed at Brookaven, New York.[19]

In 2002 a system was assembled in Brescia, Italy[20]; this unit, still at work today, is based on a JASCO J-500 electronics coupled with a low-cost grating monochromator from Optometrics, and uses an InGaAs diode detector with no need to employ a chopper to modulate the light. Figure 1 shows the schematic optical diagram, a very important feature of which is a compartment (denoted "1") that provides the possibility of getting artifact-free baselines, by placing the sample before the PEM, as originally suggested by Chabay.[21] This feature is indeed very effective in removing experimental artifacts.

NIR-VCD spectrometers considered so far (apart from the tunable laser-based one) were all of the dispersive type, i.e. they employed monochromators to vary the measurement wavelength. The design of all these types of instruments is similar. Differences may arise in the use of detectors, linear polarizers and PEMs, depending on wavelength range, which are summarized for relevant components are reported in Figure 2.

In the last 30 yr several VCD apparatuses have been proposed using interferometers and Fourier Transform techniques for the mid-IR range (800–2000 cm^{-1}) (FTIR). Today all commercially available VCD spectrometers are based on the FTIR approach. As a consequence, successful attempts were performed to extend the range of the FT-based VCD units toward the NIR range to collect high quality CD spectra of overtones.[22–24] Whether most of the well known advantages of FT are really relevant in the NIR region is an open question (the wavelength calibration assured by the automatically taken laser interferogram is substantial, but not exhaustive).

We list here few pros and cons, for the two techniques, based on the results from the two apparatuses located in Brescia, Italy, and in Syracuse, New York (referring to Refs. 22–24 for the latter one). The FT-NIR instrument covers continuously the 800–10,000 cm^{-1} range (but requires changes of the detectors and a bit of alignment as well to achieve the full range), the resolution can be pushed down to few wavenumbers, and the signal-to-noise ratio looks generally better than with dispersive instruments (except above ca. 9000 cm^{-1}), because of the possibility of fast acquisition and of averaging over large numbers of spectra. In contrast, since most NIR-VCD analyses are limited to small wavelength/wavenumber ranges, acquisition times are shorter in the dispersive modality and this may be important for the applications summarized in the Intro-

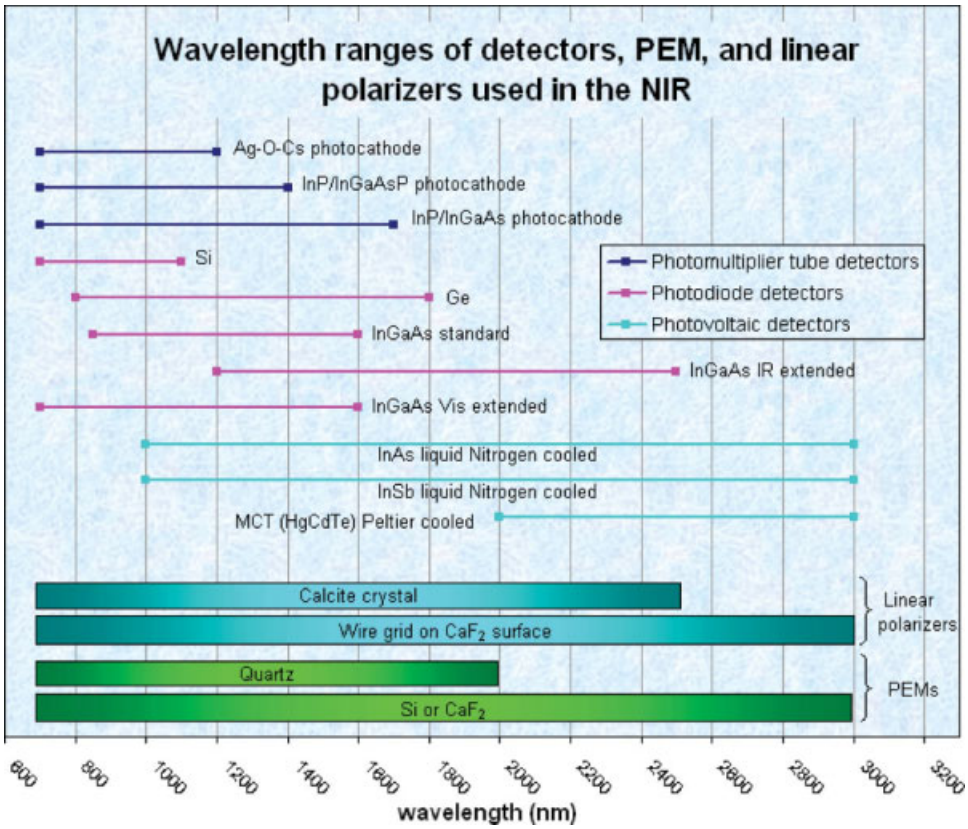

Fig. 2. Schematic representation of the various optical elements needed for the various NIR ranges with the indication of the manufacturing materials.

duction. In principle, the dispersive apparatuses allow for better use of long pathlength cells, which frequently need to be employed in the NIR. Indeed, in the FT-NIR case one is often limited by the geometry of the output beam being either divergent or too convergent, because of the use of low f/# optics. The use of very long pathlength cells is imperative for measuring NIR-VCD spectra for $\Delta v \geq 4$ CH-stretching modes. At $\Delta v = 4$ (ca. 900 nm, ca. 11,000 cm^{-1}) no FT-NIR VCD spectra have been reported yet, whereas a few examples exist from the dispersive approach[17,20] and even the $\Delta v = 5$ CH-streching overtone (ca. 760 nm, ca. 13,000 cm^{-1}) was successfully investigated[25] and recently confirmed for Limonene on the Jasco J-815SE apparatus in Brescia, employing a 19 cm pathlength cell (data not reported). To get a practical idea for the FT/dispersive comparison over a wavelength range where both types of instruments are operative, we provide in Figure 3 the NIR-VCD spectra of camphor, a compound with not too large VCD. Here spectra were taken from Ref. 24 for the FT-NIR technique and from Ref. 26 for the dispersive technique.

Although all the advantages of the interferometric technique are valid in principle over all wavelength ranges, actually there is little practical applications of this aspect of interferometry in the UV-Vis. Besides, we observe that dispersive NIR spectrophotometers are still sold by many manufacturers, even by those offering also FTIR instruments. It is perhaps useful to mention that the way in which the circularly polarized light is produced and employed in FT-NIR instruments is the same as in dispersive NIR instruments.

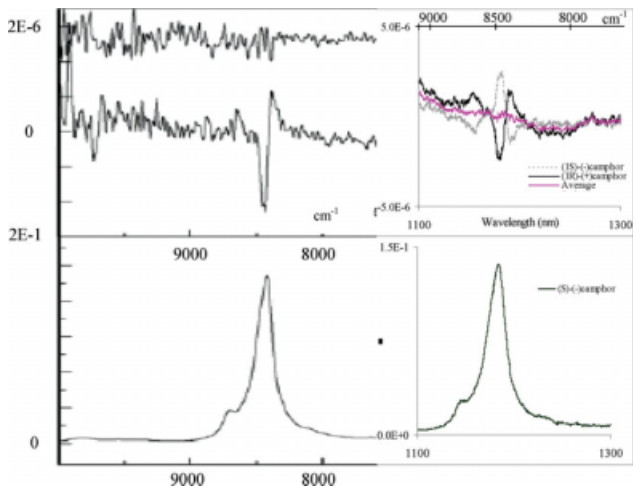

Fig. 3. Comparison of FT and dispersive NIR absorption and NIR-VCD spectra for Camphor in the CH-stretching $\Delta v = 3$ region. In the left panel we report data elaborated from Ref. 24 and on the right panel the data obtained with a dispersive instrument.[26] The FT-NIR data top trace is the noise evaluated by subtraction of identical blocks of VCD data taken at successive times (see Ref. 24). The FT-NIR VCD spectrum is just for the (1R)-enantiomer. The dispersive VCD data are for both enantiomers and we give also their arithmetic average as an evaluation of baseline and noise. As for the acquisition times, see Refs. 24 and 26.

Other possible approaches include the use of acousto-optical tuning filters, as real alternatives to conventional monochromators or interferometers: recent examples[27,28] appeared in the literature, reporting overtone ORD spectra of Camphor.

Let us list below the currently commercially available NIR CD instruments, according to the two categories discussed above: dispersive type (based on monochromators) and FTIR type (built around a Michelson interferometer). To the first category belongs the JASCO J-730 system (equipped with halogen source, grating monochromator, chopper, quartz PEM, and liquid N_2-cooled InSb detector: see www.jascoinc.com) and the Olis systems (equipped with Xenon source, multiple grating monochromators or prism-grating monochromators, quartz PEM, dual beam optics, and a pair of InGaAs detectors: see www.olisweb.-com). To the FT/NIR category belong different tailor-made variants (single or double PEM) from Bomem Bio-Tools (see www.btools.com) and dedicated NIR-CD accessories from Bruker (see www.brukeroptics.com). This list is far from being exhaustive, as other mid IR VCD manufacturers: JASCO, Nicolet (see www.thermo.com) and Varian (now part of the Agilent group) (see www.varianinc.com) could easily assemble NIR extended units on demand.

Potential users may easily follow alternative and lower cost approaches by conversion of conventional FT/NIR units to CD experiments through adding a polarizer, a suitable PEM (see www.hindspem.com) and a lock-in amplifier or a dedicated demodulation module as commercially available from GWC (see www.gwctechnologies.com) and, of course, a suitably fast detector. Following the dispersive approach, one may recycle PEM and acquisition electronics from an old CD spectrometer formerly operating in the UV-Vis range, and integrate it with a grating monochromator, a halogen source, a polarizer, and an InGaAs detector module, with built-in preamplifier as available for example from EOS (see www.eosystems.com). Home-built systems call for the availability of a local workshop and of a resident engineer willing to do the job.

The apparatus so constructed in Brescia has a maximum efficiency for the 1500–1000 nm region. This region encompasses $\Delta v = 2$ transitions for OH-stretchings ($\sim$ 1400 nm) and $\Delta v = 3$ transitions for CH-stretchings ($\sim$ 1200 nm). In Figure 4 we report spectra for enantiomeric pairs of Limonene, α-Pinene, and β-Pinene in the latter region. However Nafie et al. in the aforementioned literature[22–24] have reported also very good data for $\Delta v = 2$ CH-stretchings, as well as the (1,1) CH-stretching/HCH-bending and (2,1) CH-stretching/HCH-bending combination regions; it is worth mentioning that the (1,1) combination region was considered also in Ref. 7 and (2,1) in Ref. 20. The measurements performed so far have regarded mostly natural products, mainly terpenes, alcohols, esters,[29,30] and chiral cyclopentanone and cyclohexanone related molecules,[20] and even chiral cyclophanes.[31] A large series of molecules was also considered, for basic investigations (calibration and calculations), in Refs. 23 and 24. The epimerization of a dioxolane chiral derivative was monitored by NIR-VCD.[32] A lot remains to be done though, both for fundamental investigations and applicative goals.

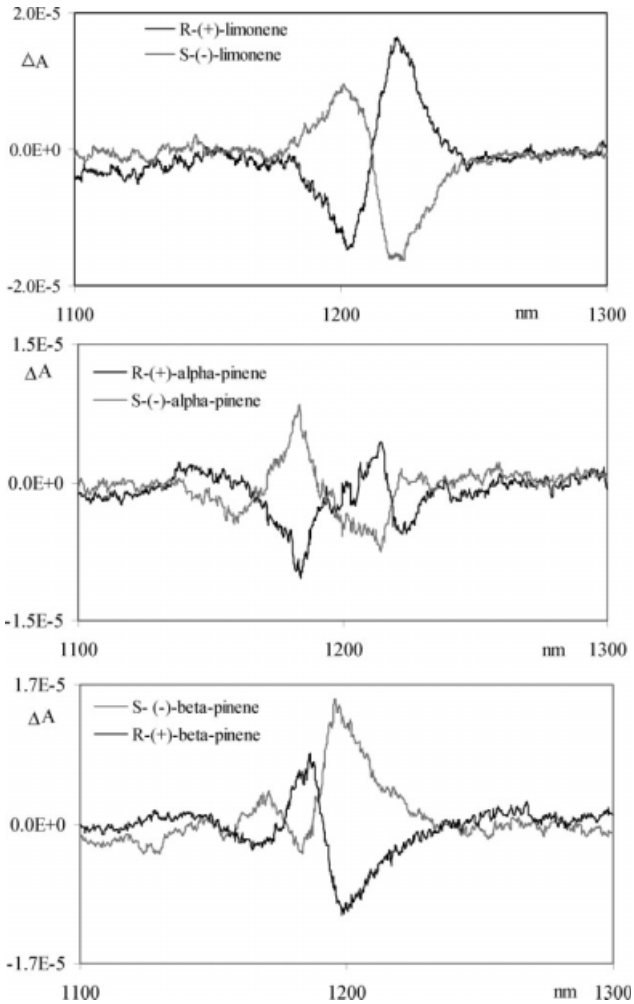

Fig. 4. Superimposed experimental NIR-VCD spectra at $\Delta v = 3$ of (*R*)-(−)-Limonene and (*S*)-(+)-Limonene (*Top Panel*); of (*R*)-(−)-β-Pinene and of (*S*)-(+)-β-Pinene (*Center Panel*); and of (*R*)-(−)-α-Pinene and of (*S*)-(+)-α-Pinene. Spectra taken on neat liquid samples contained in a 5-mm pathlength quartz cuvette.

To complete the experimental section we illustrate the sampling conditions to be adopted for running optimal NIR-VCD spectra in the different overtone regions. Dealing with pure liquids, for the $\Delta v = 2$ CH/OH stretching region (possibly containing also combination bands), between 1900 and 1300 nm (i.e. ca. between 5500 and 8000 cm^{-1}) a 1 mm cell is generally needed; for the $\Delta v = 3$ CH stretching region between 1300 and 1100 nm (i.e. ca. between 8000 and 9000 cm^{-1}) a 5 mm cell is required, whereas for the $\Delta v = 3$ OH stretching region between 1200 and 1000 nm (i.e. ca. between 8500 and 10,000 cm^{-1}) a 1 cm/2 cm (and even longer pathlength) may be required, due to the fact that the OH bond-stretching decreases in intensity with overtone order faster than the CH bond-stretching; for the the $\Delta v = 4$ CH stretching region between 1000 and 850 nm (i.e. ca. between 10,000 and 12,000 cm^{-1}) a 5 cm cell at least is needed. Dealing with solutions, one has to keep in mind the Lambert and Beer's law and may infer from the above reported pathlengths the proper pathlength for a given concentration.

The investigated neat liquids have concentrations ranging from 3 M to 6 M and the product pathlength times concentration has to be close to the values implied above. For solid samples (either in the form of pellets or films) no NIR-VCD experiment has been reported so far, to the best of our knowledge; in any case solid state sampling calls for a lot of attention to minimize potential artifacts.[33]

THEORY AND CALCULATIONS

NIR-ECD (NIR-Electronic Circular Dichroism spectra)

Before proceeding to illustrate theory and calculations for VCD in the NIR, we wish to mention important calculations that have allowed interpretation of Electronic CD spectra in the NIR (NIR-ECD). The first type of such calculations regards electronic spectra involving f or d orbitals in metal ions, in particular rare-earth ions, co-ordinated to chiral molecules, like natural products.[34,35] The second type of compounds having NIR ECD spectra are the recently investigated carbon nanotubes, either by themselves[36] or co-ordinated to DNA.[37] Such investigations had been preceded by appropriate theory[38] for highly conjugated chiral carbon systems. We mention these works here, not simply for completeness but also since involvement of low-lying electronic states has been demonstrated to be important in intensifying VCD spectra even in the IR.[39] We expect this to be valid a fortiori in the NIR.

VCD in the NIR Region

Basics to predict NIR-VCD spectra. NIR-VCD spectra contain transitions associated to overtones and combination vibrational states. Related to all these transitions, one has to evaluate three sorts of observables. The frequency or wavenumber $\omega_{\mathbf{v}}$, the rotational strength $R_{0\rightarrow\mathbf{v}}$ (and the corresponding Dipole Strength $D_{0\rightarrow\mathbf{v}}$ for the concomitant NIR absorption spectrum) and the width $\Delta\omega_{\mathbf{v}}$ of the band associated to each vibrational transition. In what follows we will concentrate on reporting advancements in calculating the first two quantities. For this we recall that to calculate the transition frequency, the mechanical vibrational problem should be solved, and that the second observable is based on the usual Rosenfeld equation[40–42]:

$$\mathrm{R}_{0\rightarrow\mathbf{v}} = Im\langle 0|\mu|\mathrm{v}\rangle \bullet \langle \mathrm{v}|m|0\rangle \qquad (1)$$

where μ is electric dipole moment operator and m is the magnetic dipole moment operator, Im stands for imaginary part, and we have used the standard braket notation of Dirac to denote the ground state $|0\rangle$ and vibrational excited state $|\mathbf{v}\rangle$, $\mathbf{v}$ being a vector, the components of which are the quantum numbers of all vibrational excitations. The corresponding intensity in absorption spectra is given by the dipole strength:

$$\mathrm{D}_{0\rightarrow\mathbf{v}} = |\langle 0|\mu|\mathrm{v}\rangle|^2 \qquad (2)$$

We will not dwell on the evaluation of $\Delta\omega_{\mathbf{v}}$, which will be empirically determined, as done also in the interpretation of mid-IR VCD spectra. For our considerations we found valuable information in two papers dealing with the bandwidth problems in NIR absorption spectra for C_6H_6 and C_6D_6 up to the $\Delta v = 10$ transition (where v is the sum of the **v**-components).[43,44] Some further help on this aspect may come from the classical/semiclassical model applicable to the molecular motion presented in Ref. 45.

When calculating $\omega_{\mathbf{v}}$ and $R_{0\rightarrow\mathbf{v}}$, two sorts of difficulties are met: (a) large number of vibrational states at increasing overtone order; (b) large anharmonic effects. Both effects are becoming manageable, especially in view of the potentialities of modern computers. In the past though these difficulties may have discouraged people from tackling the problem; recently some successful attempts have appeared in the literature to make use of ab-initio techniques.

As far as point (a) is concerned, we notice that for a molecule with n XH (most often CH) bonds, even neglecting other modes than XH-stretchings (bending deformations or CC-stretching modes), whereas the fundamental ($\Delta v = 1$) region contains n transitions, the $\Delta v = 2$ region contains $n(n+1)/2$ transitions (n overtones and $n(n-1)/2$ combinations); the $\Delta v = 3$ contains $n(n+1)(n+2)/6$ transitions: the $\Delta v = 4$ contains $n(n+1)(n+2)(n+3)/24$ transitions and so forth. For a quite studied molecule like camphor with $n = 16$, one has 16, 136, 816, and 3876 transitions, at $\Delta v = 1$, $\Delta v = 2$, $\Delta v = 3$, and $\Delta v = 4$, respectively. Conversely, a simple spectrum with just few bands is usually observed both in absorption and in VCD; this obervation has led some authors to formulate[2,3] and to theoretically justify[46,47] the local-mode approximations, whereby for $\Delta v \geq 3$ XH-stretching vibrational transitions just the n overtones transitions associated to uncoupled, i.e. local, XH-stretchings are spectroscopically active, while at $\Delta v = 1$, the n fundamental transitions regard n normal modes, which result from coupled bond stretchings, and at $\Delta v = 2$ the transitions have a mixed character. This has allowed rationalization either empirically or semiempirically/semi-ab initio of a large number of absorption NIR spectra or even of spectra obtained by nonlinear optics techniques, like photo-fragmentation spectra, two-photon spectra. Involvement of other modes, e.g. HCH overtone modes through Fermi Resonance type mechanisms have also been considered.[48]

Mechanical anharmonicities. More attention has been paid, especially in the context of VCD, to point b), as it is anharmonicity that causes the failure of the normal mode scheme at high Δv. Mechanical Anharmonicity has been and is actively studied, especially having in mind the possible perturbations to IR-VCD spectra, which are most of the times interpreted on the basis of DFT/harmonic approach,[49] with the use of packages like Gaussian03.[50] The first task is to deal with a nonharmonic Hamiltonian operator. The most used approach has been proposed for the first time, in the field of VCD, by Marcott et al.[51–53] and is based on the Van Vleck contact-transformation perturbation theory,[53–55] whereby one finds successive transformations S, allowing diagonalization of the nonharmonic Hamiltonian:

$$
\begin{aligned}
H &= H_0 + \varepsilon H_1 + \varepsilon^2 H_2 \\
H_0 &= (\mathrm{hc}/2)\sum\nolimits_{\mathrm{n}} \omega_{\mathrm{n}}[p_{\mathrm{n}}^2/\hbar^2 + q_{\mathrm{n}}^2] \\
\varepsilon H_1 &= \mathrm{hc}\sum\nolimits_{\mathrm{nml}} K_{\mathrm{nml}} q_{\mathrm{n}} q_{\mathrm{m}} q_1 \\
\varepsilon^2 H_2 &= \mathrm{hc}\sum\nolimits_{\mathrm{nmlk}} K_{\mathrm{nmlk}} q_{\mathrm{n}} q_{\mathrm{m}} q_1 q_{\mathrm{k}}
\end{aligned}
\tag{3}
$$

q_{n} being the dimensionless normal coordinate, related to normal coordinate Q_{n} (with associated harmonic frequency ω_{n}) by $q_{\mathrm{n}} = (1/\alpha_{\mathrm{n}})\, Q_{\mathrm{n}}$, where $\alpha_{\mathrm{n}} = [2\pi \mathrm{c}\omega_{\mathrm{n}}/\hbar]^{1/2}$ (h Planck's constant, $\hbar = \mathrm{h}/2\pi$ and c speed of light); $\mathrm{p_n}$ is the dimensionless moment conjugated to q_{n}, while P_{n} is conjugated to Q_{n}. This makes energies, harmonic wavenumbers ω_{n} and both cubic and quartic anharmonic force constants K_{nml} and K_{nmlk} all have the same units, namely cm^{-1}. K_{nml} and K_{nmlk} are the lowest order mechanical anharmonic parameters.

At successive orders the transformations S, solving the mechanical problem, are applied to operators like the electric and magnetic dipole moments needed for the calculations of dipole and rotational strengths (see eqns. 1 and 2). The transformed operators' transition moments are then evaluated for original harmonic wavefunctions, which depend on new contact-transformed coordinates. This approach has been made usable for ab-initio calculations by Bak et al.[56] with special attention to the ab-initio calculation of the dipole moments operators' expansions, as will be further discussed below. In the context of NIR-VCD, this formalism has been adopted by Polavarapu[57] and Abbate and coworkers.[58–60] The former author considered an isolated Morse oscillator, the latter assumed that the magnetic dipole moment can be modeled in the framework of coupled electric dipole moments. In this way they arrived at an explanation of the qualitative behavior of expected signs and intensities of calculated VCD features associated with XH overtone/combination transitions: both authors have demonstrated that the same g ratio ($g = 4\mathrm{R}/\mathrm{D}$, R and D being respectively the rotational and dipole strength associated with the transition under study) is expected for fundamental and overtone transition.

Schematically, if one wishes to run full ab-initio calculations of NIR-VCD spectra, one needs to tackle four problems, two of which consist in dealing with mechanical anharmonicity, and two consist in dealing with electrical and magnetic anharmonicities:

(i) Calculations of anharmonic force constants K_{nml} and K_{nmlk} appearing in eq. 3. Recently Barone[61] has provided a general methodology for the calculation of a complete set thereof and implemented it in the GAUSSIAN03 package.[50] However we wish to say that for the NIR region a good and a more economic alternative to that approach for just XH-stretchings has been suggested and practiced by Kjaergaard and coworkers[62,63]; by the latter procedure one calculates via DFT ω_{n} as $(K_{\mathrm{nn}}/m)^{1/2}$ by analytical second derivative and K_{nnn} and K_{nnnn} by opportunely stretching the XH bond and by polynomial interpolation of the calculated energy function. Therefrom one gets the anharmonicity constant from the relation[63,64]:

$$
\chi_n = \frac{h}{64\pi^2 mc}\left(\frac{5}{3}\frac{K_{\mathrm{nnn}}^2}{K_{\mathrm{nn}}^2} - \frac{K_{\mathrm{nnnn}}}{K_{\mathrm{nn}}}\right) \tag{4}
$$

so that the anharmonic v-th overtone ω_{nv} is given by:

$$
\omega_{\mathrm{nv}} = hc\left(\omega_n\left(v+\frac{1}{2}\right) - \chi_n\left(v+\frac{1}{2}\right)^2\right) \tag{5}
$$

The application to chiral molecules is reported in Ref. 65.

(ii) Calculating the S generating function at various orders from knowledge of K_{ijk} and K_{ijkl} is the second step. The general formulae date back to the Van Vleck-Nielsen school[54,55] and are given, for the VCD context, among others, by Marcott et al.[51–53] and by Bak et al.[56] However quite efficient procedures to apply these transformations to multidimensional problems are to be sought carefully, to decrease computation time and to increase precision. We find that writing the S functions in terms of creation and destruction operators, so as to be able to apply Wick's ordering theorem results in fast diagonalization, as demonstrated by Sibert[66] for the CH-stretching high overtone absorption case. We applied that method with empirical parameters to the calculation of overtone VCD spectra for an asymmetric HCCH fragment.[60]

Electrical and magnetic anharmonicities. Below let us briefly illustrate the two steps regarding the calculations Electrical and Magnetic Anharmonicities and combining their effects with those from Mechanical Anharmonicity.

(i) Evaluation of non-harmonic dipole moment operators. The latter operators, needed in eq. 1, are to be expanded beyond the harmonic approximation, and the expansion coefficients can be calculated ab initio or via DFT, as proposed by Bak et al.[56] or by F. Gangemi et al.[65,67] By defining μ_i and m_i being the three Cartesian components (i = x,y,z) of the electric and magnetic dipole moment operators respectively one has:

$$
\begin{aligned}
\mu_i = &\sum_n \sum_{\alpha j} \prod\nolimits^0_{\alpha ij} \frac{L^n_{\alpha j}}{\sqrt{m_{\mathrm{G}}}} Q_n \\
&+ \frac{1}{2}\sum_n \sum_{\alpha j \beta k}\left(\frac{\partial \prod_{\alpha ij}}{\partial R_{\beta k}}\right)_0 \frac{L^n_{\alpha j} L^n_{\beta k}}{m_{\mathrm{G}}} Q_n^2 \\
&+ \frac{1}{6}\sum_n \sum_{\alpha j \beta k \gamma l}\left(\frac{\partial^2 \prod_{\alpha ij}}{\partial R_{\beta k}\partial R_{\gamma l}}\right)_0 \frac{L^n_{\alpha j} L^n_{\beta k} L^n_{\gamma l}}{(m_{\mathrm{G}})^{3/2}} Q_n^3 + \cdots
\end{aligned}
\tag{6}
$$

$$
\begin{aligned}
m_i = &\, 2\hbar \sum_n \sum_{\alpha j} A^0_{\alpha ij} \frac{L^n_{\alpha j}}{\sqrt{m_{\mathrm{G}}}} P_n \\
&+ 2\hbar \sum_n \sum_{\alpha j \beta k}\left(\frac{\partial A_{\alpha ij}}{\partial R_{\beta k}}\right)_0 \frac{L^n_{\alpha j} L^n_{\beta k}}{m_{\mathrm{G}}} Q_n P_n \\
&+ \frac{1}{2}\hbar \sum_n \sum_{\alpha j \beta k \gamma l}\left(\frac{\partial^2 A_{\alpha ij}}{\partial R_{\beta k}\partial R_{\gamma l}}\right)_0 \frac{L^n_{\alpha j} L^n_{\beta k} L^n_{\gamma l}}{(m_{\mathrm{G}})^{3/2}} (Q_n^2 P_n - Q_n^2 P_n) + \cdots
\end{aligned}
\tag{7}
$$

The atomic polar tensors (APT) and the atomic axial tensors (AAT), respectively,[49,56] are here considered as functions of nuclear positions and expanded around the equilibrium geometry. So in eqs. 6 and 7 the APT relative to atom α: $\prod^0_{\alpha ij} = \partial\mu_i/\partial R_{\alpha j}$, and the AAT for the same atom, $A^0_{\alpha ij}$, appear together with their first and second order derivatives with respect to Cartesian nuclear coordinates $R_{\beta k}$. The derivatives of APT and AAT are precisely the parameters that define the electrical and magnetic anharmonicities, respectively. The coefficients $L^n_{\alpha j}$ relate the normal coordinate Q_n to the j-th Cartesian component of the atomic displacement of atom α. m_G is defined in Ref. 67 as a mass-normalizing constant. This third step is in general lengthy, but may be simplified by replacing Cartesian coordinates with suitable internal coordinates, as has been done in a real local mode case,[65] as well as in another case, where the existence of local modes has been assumed.[67]

(ii) Finally, the S functions are applied to the electric and magnetic dipole moment operators of eqs. 6 and 7, affecting coordinates Q_n and momenta P_n appearing there. After this, one takes their transition moments between unperturbed wavefunctions, formally depending on the "new" coordinates and momenta. This last point is straightforward, since the transition moments of simple polynomials as those appearing in eq. 6 and 7, for transitions 0→v are known and tabulated (see the Appendix of Ref. 67).

The program, composed of all steps illustrated earlier, has not yet been carried out in general, mainly because of the difficulties in steps (ii) of Mechanical Anharmonicities section and Electrical and magnetic anharmonicities section and to the long time taken by the calculation of all anharmonic parameters. The solution of these problems on simple model systems leads one to understand the transition from the normal mode to the local mode regime and to understand how it happens that only pure overtones bear intensity.[59,60]

In simple cases there is no doubt that modes are local, as e.g. when there is just one single XH bond in the molecule under study. This is the case of the OH bond in alcohols; additionally bicyclic compound-based alcohols, like e.g. (*1R*)-(+)-endo-borneol and (1*S*)-(−)-endo-borneol or (1*R*)-(+)-endo-fenchyl alcohol, possess a limited number of conformations (essentially three). For these cases one may skip step (ii) of Mechanical Anharmonicities and may assume the OH-stretching normal mode Q to be defined by two atomic motions, the motion of O being (m_H/m_O) times the motion of H. Calculations of APTs and AATs and their derivatives in eqs. 6 and 7 regard just these two atoms. In step (ii) of Electrical and magnetic anharmonicities one uses then Morse wavefunctions, which are univocally determined by ω_n and χ_n, as calculated in step (i) of Mechanical Anharmonicities. The results are given in Figure 5 for the $\Delta v = 2$ region for (*1S*)-(−)-*endo*-borneol[65] and (*1S*)-endo-fenchyl alcohol. A first study of basis set influence on NIR-VCD calculations is given here: two basis sets, namely 6-31G** and 6-311++G** have been employed with the same functional B3LYP. The latter choice provides us with slightly better results, even though the calculated frequencies are overestimated. The crucial difference in the two sets of calculations is in the value of the mechanical frequency ω_n for the three rotameric states of the OH-bond in the two molecules (see Table 1). The calculated values of χ_n and of the electric and magnetic parameters (APT and AAT and their derivatives) are less important for the overall prediction. At this point we need to say that this simplified procedure, that relies on the local mode assumption, gives very good results also for (*1S*)-camphor and (*1S*)-camphorquinone at $\Delta v = 2$ and $\Delta v = 3$, as of Figure 6.[67] To go beyond the local mode assumption, further work needs to be done with full consideration of all the four steps of paragraphs Mechanical Anharmonicities and Electrical and magnetic anharmonicities.

Anharmonic non-Born Oppenheimer terms. As a last comment we wish to reconsider eq. 7, that had been justified by Bak et al.,[56] having in mind that further non Born Oppenheimer (BO) terms may play a role in overtones and combinations that had not been considered in dealing with fundamentals. Let us make a short digression for this purpose. To calculate appropriate wavefunctions for the evaluation of magnetic dipole transition moments, consider a vibrational state related to the electronic ground state. The BO expansion may be written as follows (making use of the suggestions from Refs. 56,68):

$$\begin{aligned}\Psi_{0\alpha} &= \phi_0\chi_{0\alpha} + \sum_{k\gamma\neq 0\alpha} \frac{\langle \phi_k\chi_{k\gamma}|T_{N2}|\phi_0\chi_{0\alpha}\rangle}{E_{0\alpha}-E_{k\gamma}}\phi_k\chi_{k\gamma} \\ &= \phi_0\chi_{0\alpha} + \sum_{\gamma\neq\alpha} \frac{\langle \phi_0\chi_{0\gamma}|T_{N2}|\phi_0\chi_{0\alpha}\rangle}{E_{0\alpha}-E_{0\gamma}}\phi_0\chi_{0\gamma} \\ &\quad + \sum_{k\neq 0}\sum_{\gamma} a_{k\gamma 0\alpha}\phi_k\chi_{k\gamma} + \sum_{k\neq 0}\sum_{\gamma} a^{corr}_{k\gamma 0\alpha}\phi_k\chi_{k\gamma} \end{aligned} \quad (8)$$

where ϕ_k and $\chi_{k\gamma}$ are the electronic and vibrational part, respectively, of the wavefunction of level (k,γ) in the BO approximation. T_{N2} is defined by the equation:

$$T_{N2}\phi_k\chi_{k\alpha} = -\left(\sum_{\lambda i}\frac{\hbar^2}{2M_\lambda}\frac{\partial^2\phi_k}{\partial R^2_{\lambda i}}\right)\chi_{i\alpha} - \sum_{\lambda i}\frac{\hbar^2}{M_\lambda}\frac{\partial\phi_k}{\partial R_{\lambda i}}\frac{\partial\chi_{k\alpha}}{\partial R_{\lambda i}}$$

The coefficient $a_{k\gamma 0\alpha}$ appearing in eq. 8 is:

$$a_{k\gamma 0\alpha} = \frac{\langle \phi_k\chi_{k\gamma}|T_{N2}|\phi_0\chi_{0\alpha}\rangle}{E_0(R)-E_k(R)} \quad (9)$$

and had been previously considered by Bak et al.,[56] with the explicit dependence on the geometry off-equilibrium, under the BO approximation, to keep track of anharmonicity. The coefficient $a^{corr}_{k\gamma 0\alpha}$ in the next term is given by:

$$a^{corr}_{k\gamma 0\alpha} = \frac{\langle\chi_{k\gamma}|\langle\phi_k|T_{N2}|\phi_0\rangle|\chi_{0\alpha}\rangle}{(E_0-E_k)^2}[E_{k\gamma}-E_k-(E_{0\alpha}-E_0)] \quad (10)$$

and is the first term beyond the approximation considered in Refs. 56, 65, 67.

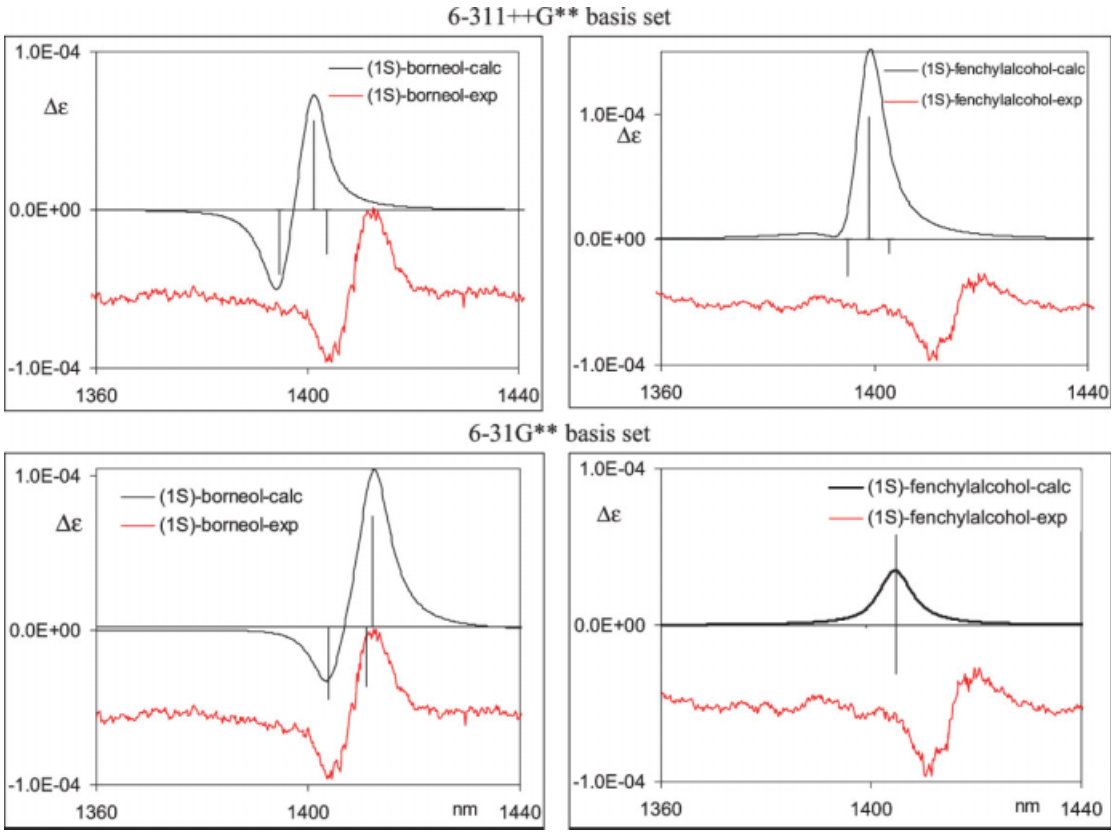

Fig. 5. Comparison of experimental (red) and calculated (black) NIR-VCD spectra of (*1S*)-(−)-*endo*-borneol (*Left Panel*) and (*1S*)-(−)-fenchyl alcohol (*Right Panel*) at $\Delta v = 2$ for the OH-stretching. Two different basis sets used for the calculations. The experimental spectrum of (*1S*)-(−)-*endo*-borneol is from Ref. 65; the experimental spectrum of (*1S*)-(−)-fenchyl alcohol is obtained by reversing the sign of the original spectrum obtained on (*1R*)-(+)-fenchyl alcohol with the same apparatus and protocol described in Ref. 65. The calculations are conducted with the procedure described in the text and rotational strengths are weighted according to Gibbs free energy. Lorentzian band-shape in wavenumber assumed with $\Delta\omega = 20$ cm^{-1}, corresponding to $\Delta\lambda \approx 4$ nm. Rotational strengths, represented by black bars, are in arbitrary units.

In the second step of eq. 8, the part of summation with $k = 0$ has been isolated, as it does not contribute to the calculation of the magnetic moment, as discussed by Bak et al.[56] and by Stephens.[49] The energy terms in the denominator of eqs. 9 and 10 are functions of the molecular geometry, either at equilibrium or off-equilibrium. Exploiting this dependence, the third term in the second step of eq. 8 has been shown to provide magnetic anharmonicity to the magnetic dipole moment. Instead, the fourth term in the second step of eq. 8 has never been considered previously. Following Ref. 68 it can be shown that the corresponding correction to the transition dipole moment is of the same order of magnitude as the anharmonic corrections coming from the expansion of the potential up to fourth order and from the expansions of the atomic axial and polar tensors as reported in eqs 6 and 7, so that it turns out to be relevant starting at $\Delta v = 3$. This correction may be calculated by explicit consideration of the coefficients $a^{\text{corr}}_{k\gamma 0\alpha}$ given in eq. 10 and may be written, similarly to what done in Ref. 56 for the lowest order term, as

TABLE 1. Calculated mechanical harmonic and anharmonic parameters for (*1S*)-borneol and (*1S*)-fenchylalcohol in their three conformational states, obtained by two different Gaussian basis sets. The numbering of carbon atoms for the definition of the dihedral angles in the table follows the chemical notation

	Borneol							Fenchylalcohol					
	τ (HOC_2C_1)		ω (cm^{-1})		χ (cm^{-1})			τ (HOC_2C_1)		ω (cm^{-1})		χ (cm^{-1})	
	*631G***	*6311 ++G***	*6-31G***	*6311 ++G***	*6-31G***	*6311 ++G***		*631G***	*6311 ++G***	*6-31G***	*6311 ++G***	*6-31G***	*6311 ++G***
1	68	74	3809	3834	88.6	88.6	1	60	60	3818	3830	89.3	88.6
2	175	170	3823	3845	86.8	86.6	2	−68	−73	3826	3847	88.1	87.7
3	−72	−68	3813	3827	90.0	88.2	3	−175	−169	3816	3840	88.5	88.7

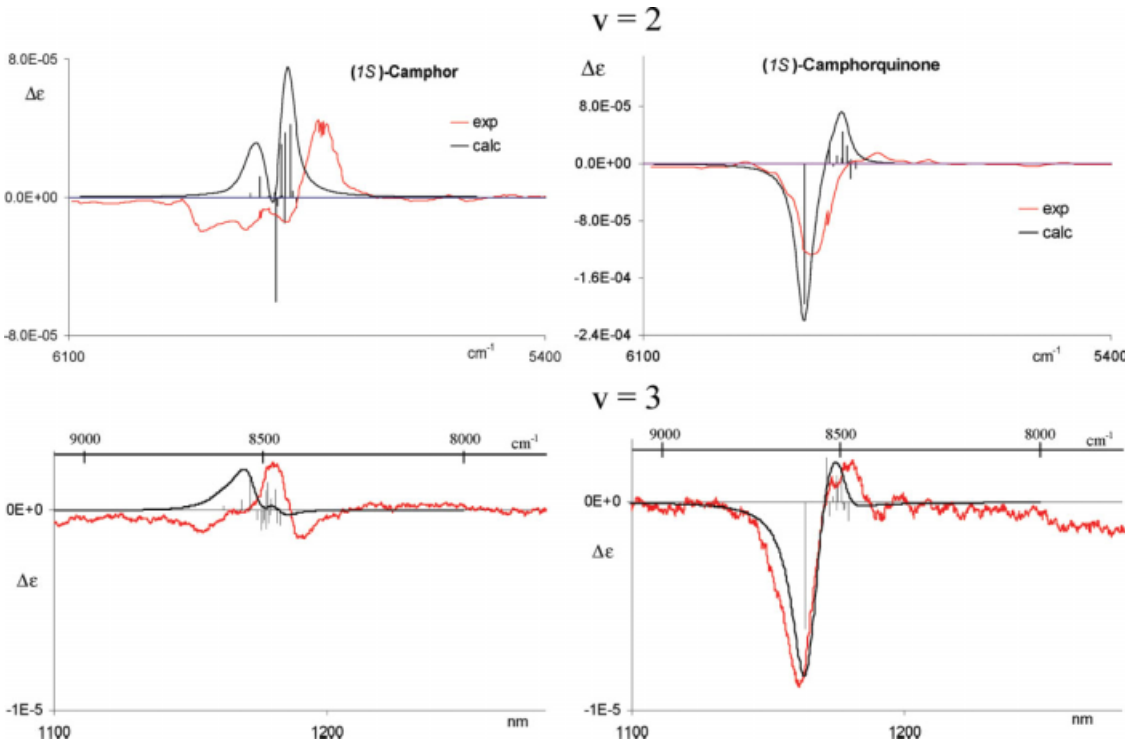

Fig. 6. Comparison of experimental (red) and calculated (black) NIR-VCD spectra of (*1S*)-(+)-camphor (left) and (*1S*)-(−)-camphorquinone (right) at $\Delta v = 2$ for the CH-stretchings (Top) and at $\Delta v = 3$ for the CH-stretchings (Bottom). The calculations are conducted as described in the text and in Ref. 67; note that χ is taken from experimental data. Lorentzian band-shapes in wavenumbers assumed with corresponding values $\Delta\lambda \approx 5$ nm at $\Delta v = 2$ and $\Delta\lambda \approx 7$ nm at $\Delta v = 3$. Data at $\Delta v = 2$ taken and redrawn from Ref. 24. Rotational strengths, represented by black bars, are in arbitrary units.

$$\langle m_i \rangle_{\mathrm{corr}} = \langle \chi_{0v} | m_{i,00}^{e,\mathrm{corr}} | \chi_{00} \rangle - \langle \chi_{00} | m_{i,00}^{e,\mathrm{corr}} | \chi_{0v} \rangle$$

where, with some algebra that we do not report here, one may show that:

$$m_{i,00}^{e,\mathrm{corr}} = \sum_{k \neq 0} \left[\frac{\langle \phi_0 | m_i^e | \phi_k \rangle}{(E_0 - E_k)^2}, T_{\mathrm{N}} \right] \langle \phi_{\mathrm{k}} | T_{\mathrm{N2}} | \phi_0 \rangle \qquad (11)$$

T_{N} is the usual full nuclear kinetic energy operator and the square brackets in eq. 11 mean commutation. We have not yet been able to reconcile eq. 11 with the response of the molecular energy contribution from higher order terms in a constant magnetic field **B**, as done at first order for the first terms, leading to eq. 7. We only observe that, because of the presence of T_{N} and T_{N2} operators, these correction terms may allow for the presence of $p_{\lambda l}^2$ and $p_{\lambda l}^3$ terms, as pointed out some time ago by Polavarapu.[57] These terms are relevant for overtone magnetic dipole transition moments for $\Delta v = 3$ and further.

SUMMARY AND CONCLUSIONS

We have reviewed the measurements of NIR-VCD spectra made so far and have described the experimental apparatuses designed and employed to this purpose. We have also presented the current status of theory and calculations needed to interpret the NIR-VCD spectra. We foresee a wealth of applications of NIR-VCD spectroscopy, as so many applications have already been proposed for mere absorption NIR spectroscopy; we also point out many interesting theoretical problems tied to the non harmonic character of the calculations necessary to reproduce NIR-VCD experimental spectra. We hope that this mini-review may arouse some curiosity and may motivate young researchers to enter the field of NIR-VCD spectroscopy.

LITERATURE CITED

1. Siesler HW, Ozaki Y, Kawata S, editors. Near infrared spectroscopy. Principles, instruments, applications. Wiley-VCH, Weinheim, Germany, 2002.
2. Child MS, Halonen L. Overtone frequencies and intensities in the local mode picture. Adv Chem Phys 1985;57:1–58.
3. Henry BR, The local mode model and overtone spectra: a probe of molecular structure and conformation. Acc Chem Rev 1987;20:429–435.
4. Sage ML, Jortner J, Bond Modes. Adv Chem Phys 1981;47:293–322.
5. Fang HL, Swofford RL, McDevitt M, Anderson AB. CH stretching overtone spectrum of propylene: molecular orbital analysis in the local-mode model. J Phys Chem. 1985;89:225–229.
6. Vaida V, Daniel JS, Kjaergaard HG, Gross LM, Tuck F. Atmospheric absorption of near infrared and visible solar radiation by the hydrogen bonded water dimer. Quart J Royal Metereol Soc 2001;127:1627–1644.
7. Keiderling TA, Stephens PJ. Vibrational circular dichroism of overtone and combination bands. Chem Phys Lett 1976;41:46–48.
8. Grosjean M, Legrand M. Appareil de mesure du dichroisme circulaire dans le visible et l'ultraviolet. Compt Rend Acad Sci 1960;251:2150–2153.

9. Abu-Shumays A, Cook RB. SCSAS Eigth Pacific Conf. Anaheim, California, Oct 1969.
10. Eaton WA, Lovenberg W. Near-infrared circular dichroism of an iron-sulfur protein. d-d transitions in rubredoxin. J Am Chem Soc 1970;92:7195–7198.
11. Grinter R, Harding MJ, Mason SF. Optical rotary power of coordination compounds Part XIV crystal spectrum and circular dichroism of α-Ni$(H_2O)_6SO_4$. J Chem Soc (A) 1970;667–671.
12. Russel MF, Billardon M, Badoz JP. Circular and linear dichrometer for the near infrared. Appl Opt 1972;11:2375–2378.
13. Chabay I, Hsu EC, Holzwarth G. Infrared circular dichroism measurement between 2000 and 5000 cm-1: Pr3+-tartrate complexes Chem Phys Lett 1972;15:211–214.
14. Osborne GA, Cheng JC, Stephens PJ. A near-infrared circular dichroism and magnetic circular dichroism instrument. Rev Sci Instrum 1973;44:10–15.
15. Koehler ME, Urbach FL. A microprocessor controlled near-infrared circular dichroism spectrometer. Appl Spectr 1979;33:563–569.
16. Nozawa T, Takao Y, Hatano M. Infrared magnetic circular dichroism of myoglobin derivatives. Biochim Biophys Acta 1976;427:28–37.
17. Abbate S, Longhi G, Ricard L, Bertucci C, Rosini C, Salvadori P, Moscowitz A. Vibrational circular dichroism as a criteria for local-mode versus normal-mode behavior. Near-infrared circular dichroism of some monoterpenes. J Am Chem Soc 1989;111:836–840.
18. Tran CD, Grishko VI. Universal spectropolarimeter based on overtone circular dichroism measurements in the near-infrared region. Anal Chem 1994;66:3639–3643.
19. Olson JM, Trunk J, Sutherland JC. Circular dichroism of the 1300-nm band of oxidized reaction centers from rhodopseudomonas viridis. Biochem 1985;24:4495–4499.
20. Castiglioni E, Lebon F, Longhi G, Abbate S. Vibrational circular dichroism in the near infrared: instrumental developments and applications. Enantiomer 2002;7:161–173.
21. Chabay I. Infrared circular dichroism measurements, PhD Thesis, University of Chicago, 1972.
22. Nafie LA, Dukor RK, Roy JR, Rilling A, Cao X, Buijs H. Observation of Fourier transform near-infrared vibrational circular dichroism to 6150 cm^{-1}. Appl Spectrosc 2003;57:1245–1249.
23. Cao X, Shah RD, Dukor RK, Guo C, Freedman TB, Nafie LA. Extension of Fourier transform vibrational circular dichroism into the near-infrared region: continuous spectral coverage from 800 to 10 000 cm^{-1}. Appl Spectrosc 2004;58:1057–1064.
24. Guo C, Shah RD, Dukor RK, Freedman TB, Cao X, Nafie LA. Fourier transform vibrational circular dichroism from 800 to 10,000 cm^{-1}: near-ir-VCD spectral standards for terpenes and related molecules. Vibr Spectrosc 2006;42:254–272.
25. Abbate S, Longhi G, Givens JW III, Boiadjiev S, Lightner DA, Moscowitz A. Observation of vibrational circular dichroism for overtone transitions with commercially available CD spectrometers. Appl Spectrosc 1996;50:642–643.
26. Longhi G, Gangemi R, Lebon F, Castiglioni E, Abbate S, Pultz VM, Lightner DA. A comparative study of overtone CH-stretching vibrational circular dichroism spectra of fenchone and camphor. J Phys Chem A 2004;108:5338–5352.
27. Chen Z, Khurgin J, Lorenzo J, Jin F, Xlong X, Jla K, Trivedi S, Soos J, Hansen M, Russomanno C. Near-infrared spectropolarimeter using an acousto-optic tunable filter. Optl Engin 2007;46:073605-1–6.
28. Fernandes Pereira C, Barbieri Gonzaga F, Pasquini C. Near-infrared spectropolarimeter based on acousto-optical tunable filters. Anal Chem 2008;80:3175–3181.
29. Nakao Y, Sugeta H, Kyogoku Y. Vibrational circular dichroism of the OH stretching vibrations in methyl 3-hydroxybutyrate and methyl lactate. Chem Lett 1984;623–626.
30. Yamamoto K, Nakao Y, Kyogoku Y, Sugeta H, Vibrational circular dichroism in hydrogen bond systems: Part III. Vibrational circular dichroism of the OH stretching vibrations of 1,2-diols and β-methoxyalcohols J Mol Struct 1991;242:75–86.
31. Abbate S, Castiglioni E, Gangemi F, Gangemi R, Longhi G, Ruzziconi R, Spizzichino S. Harmonic and anharmonic features of IR and NIR absorption and VCD Spectra of Chiral 4-X-[2.2]paracyclophanes. J Phys Chem A 2007;111:7031–7040.
32. Guo C, Shah RD, Mills J, Cao X, Freedman TB, Nafie LA. Fourier transform near-infrared VCD used for on-line Monitoring the epimerization of 2,2-dimethyl-1,3-dioxolane-4-methanol: a pseudo racemization reaction. Chirality 2006;18:775–782.
33. Castiglioni E, Biscarini P, Abbate S. Experimental aspects of solid state circular dichroism. Chirality 2009. DOI: 10.1002/chir. 20770.
34. Salvadori P, Rosini C, Bertucci C. Near-infrared f-f transition Cotton effects of ytterbium(III) ion: experimental evidences for interaction between rifamycin antibiotics and metal ions. J Am Chem Soc 1984;106:2439–2440.
35. Di Bari L, Pintacuda G, Salvadori P, Dickins RS, Parker D. Effect of axial ligation on magnetic and electronic properties of lanthanide complexes of octadentate ligands. J Am Chem Soc 2000;122:9257–9264.
36. Dukovic G, Balaz M, Doak P, Berova ND, Zheng M, McIean RS, Brus LE. Racemic single-walled carbon nanotubes exhibit circular dichroism when wrapped with DNA. J Am Chem Soc 2006;128:9004–9005.
37. Peng X, Komatsu N, Bhattacharya S, Shimawaki T, Aonuma S, Kimura T, Osuka A. Optically active carbon nanotubes. Nat Nanotechnol 2007;2:361–365.
38. Nunzi F, Mercuri F, Sgamellotti A, Re N. The coordination chemistry of carbon nanotubes: a density functional study through a cluster model approach. J Phys Chem B, 2002;106:10622–10633.
39. Freedman TB, Xiaolin C, Young DA, Nafie LA. Density functional theory calculations of vibrational circular dichroism in transition metal complexes: identification of solution conformations of chloride ion association for (+)-tris(ethylendiaminato)cobalt(III). J Phys Chem A 2002;106:3560–3565.
40. Rosenfeld R. Quantenmechanische Theorie der natürlichen optischen Aktivität von Flüssigkeiten und Gasen. Z Phyz 1928;52:161–174.
41. Condon U. Theories of optical rotatory power. Rev Modern Phys 1937;9:432–457.
42. Condon U, Altar W, Eyring M, One Electron Rotatory Power. J Chem Phys 1937;10:753–774.
43. Reddy KV, Heller DF, Berry MJ. Highly vibrationally excited benzene: overtone spectroscopy and intramolecular dynamics of C_6H_6, C_6D_6 and partially deuterated or substituted benzenes. J Chem Phys 1982;76:2814–2837.
44. Sibert EL III, Reinhardt WP, Hynes JT. Intramolecular vibrational relaxation and spectra of CH and CD overtones in benzene and perdeutero benzene. J Chem Phys 1984;81:1115–1134.
45. Abbate S, Longhi G, Kwon K, Moscowitz A. The use of cross-correlation functions in the analysis of circular dichroism spectra. J Chem Phys 1998;108:50–62.
46. Lehmann KK. On the relation of Child and Lawton's harmonically coupled anharmonic-oscillator model and Darling-Dennison coupling. J Chem Phys 1983;79:1098.
47. Mills IM, Robiette AG. On the relationship of normal modes to local modes in molecular vibrations. Mol Phys 1985;56:743–765.
48. Ricard-Lespade L, Longhi G, Abbate S. The first overtone of CH stretching in polymethylene chains: a conformationally dependent spectrum. Chem Phys 1990;142:245–253.
49. Stephens PJ. The theory of vibrational circular dichroism. J Phys Chem 1985;89:748–750.
50. Gaussian 03, Revision B. 05, Frisch MJ, Trucks GW, Schlegel HB, Scuseria GE, Robb MA, Cheeseman JR, Montgomery JA Jr, Vreven T, Kudin KN, Burant JC, Millam JM, Iyengar SS, Tomasi J, Barone V, Mennucci B, Cossi M, Scalmani G, Rega N, Petersson GA, Nakatsuji H, Hada M, Ehara M, Toyota K, Fukuda R, Hasegawa J, Ishida M, Nakajima T, Honda Y, Kitao O, Nakai H, Klene M, Li X, Knox JE, Hratchian HP, Cross JB, Bakken V, Adamo C, Jaramillo J, Gomperts R, Stratmann RE, Yazyev O, Austin AJ, Cammi R, Pomelli C, Ochterski JW, Ayala PY, Morokuma K, Voth GA, Salvador P, Dannenberg JJ, Zakrzewski VG, Dapprich S, Daniels AD, Strain MC, Farkas O, Malick DK, Rabuck AD, Raghavachari K, Foresman JB, Ortiz JV, Cui Q, Baboul AG, Clifford S, Cioslowski J, Stefanov BB, Liu G, Liashenko A,

Piskorz P, Komaromi I, Martin RL, Fox DJ, Keith T, Al-Laham M. A, Peng CY, Nanayakkara A, Challacombe M, Gill PMW, Johnson B, Chen W, Wong MW, Gonzalez C, Pople JA. Gaussian, Inc., Wallingford CT, 2004.

51. Marcott C. Vibrational circular dichroism and the structure of chiral Molecules, PhD Thesis, University of Minnesota, 1976.
52. Faulkner TR, Marcott C, Moscowitz A, Overend J. Anharmonic effects in vibrational circular dichroism. J Am Chem Soc 1977;99:8160–8169.
53. Marcott C, Faulkner TR, Moscowitz A, Overend J. Vibrational circular dichroism in bromochlorofluoromethane and bromochlorofluoromethane-d. Calculation of the rotational strengths associated with the fundamentals and the binary overtones and combinations. J Am Chem Soc 1977;99:8169–8175.
54. Amat G, Nielsen HH, Tarrago G. Rotation-vibration od Polyatomic Molecules. M. Dekker Inc, New York, 1971.
55. Nielsen HH, The Vibration-Rotation Energies of Polyatomic Molecules Part II. Accidental Degeneracies, Phys Rev 1945;68:181–191.
56. Bak KL, Bludskỳ O, Jørgensen P. Ab initio calculations of anharmonic vibrational circular dichroism intensities of trans-2,3-dideuterio-oxirane. J Chem Phys 1995;103:10548–10555.
57. Polavarapu PL. Vibrational optical activity of anharmonic oscillator Mol Phys 1996;89:1503–1510.
58. Abbate S, Longhi G, Santina C. Theoretical and experimental studies for the interpretation of vibrational circular dichroism spectra in the CH-stretching overtone region. Chirality 2000;12:180–190.
59. Abbate S, Gangemi R, Longhi G. Dipole and rotational strengths for overtone transitions of a C_2-symmetry HCCH molecular fragment using Van Vleck perturbation theory. J Chem Phys 2002;117:7575–7586.
60. Gangemi R, Longhi G, Abbate S. Calculated absorption and vibrational circular dichroism spectra of fundamental and overtone transitions for a chiral HCCH fragment in the hypothesis of coupled dipoles. Chirality 2005;17:530–539.
61. Barone V, Aharmonic vibrational properties by a fully automated second-order perturbative approach. J Chem Phys 2005;122:014108/1–014108/10.
62. Kjaergaard HG, Henry BR, The relative intensity contributions of axial and equatorial CH bonds in the local mode overtone spectra of cyclohexane. J Chem Phys 1991;96:4841–4851.
63. Howard DA, Jørgensen P, Kjaergaard HG. Weak intramolecular interactions in ethylene glycol identified by vapor phase OH-stretching overtone spectroscopy. J Am Chem Soc 2005;127:17096–17103.
64. Halonen L, Local mode vibrations in polyatomic molecules. Adv Chem Phys 1998;104:41–179.
65. Gangemi F, Gangemi R, Longhi G, Abbate S. Experimental and ab-initio calculated spectra of the first OH-streching overtone of (1R)-(-)-endo-Borneol and (1S)-(+)-endo-Borneol. Phys Chem Chem Phys, 2009;11:2683–2689.
66. Sibert EL III. Theoretical studies of vibrationally excited polyatomic molecules using Van Vleck perturbation theory. J Chem Phys 1988;88:4378–4390.
67. Gangemi F, Gangemi R, Longhi G, Abbate S. Calculations of overtone NIR and NIR-VCD Spectra of camphor and camphorquinone in the local mode approximation. Vibrational Spectroscopy 2009;50:257–267.
68. Mead CA, Moscowitz A. Dipole length versus dipole velocity in the calulation of Infrared intensities with Born-Oppenheimer wave functions. Int J Quantum Chem 1967;1:243–249.